Evolution of Anisotropic Diffusion in the Developing Rat Corpus Callosum

IVAN VOŘÍŠEK[1] AND EVA SYKOVÁ[1,2]
[1]*Department of Neuroscience, Institute of Experimental Medicine, Academy of Science of the Czech Republic, Prague 142 20; and* [2]*Department of Neuroscience, Second Medical Faculty, Charles University, Prague 150 18, Czech Republic*

Voříšek, Ivan and Eva Syková. Evolution of anisotropic diffusion in the developing rat corpus callosum. *J. Neurophysiol.* 78: 912–919, 1997. Diffusion anisotropy was investigated in the developing rat brain [postnatal day (P)6–29] with the use of ion-selective microelectrodes to measure the three-dimensional distribution of tetramethylammonium (TMA^+) iontophoresed into the extracellular space (ECS). The diffusion parameters, ECS volume fraction α (α = ECS volume/total tissue volume), tortuosity λ (λ^2 = apparent diffusion coefficient/free diffusion coefficient), and nonspecific TMA^+ uptake (k'), were studied in cortical gray matter (layer V) and corpus callosum (CC) of anesthetized rats. ECS volume fraction in cortex and CC was about twice as large in the newborn rat as in adults. In this study, more detailed analysis revealed that α in CC gradually decreased from P4, when α ranged between 0.42 and 0.45, and reached a final value of 0.26 ± 0.01 (SE, n = 12 measurements, 6 animals) at about P21. Diffusion in the ECS of CC was isotropic until about P12, i.e., there was no significant difference in the tortuosity factor, λ, between the three perpendicular axes. From P13 to P17 anisotropy greatly increased as a result of preferential diffusion along the myelinated axons (X-axis). At P21–23 the tortuosity values were λ_x = 1.46 ± 0.03, λ_y = 1.70 ± 0.01, and λ_z = 1.72 ± 0.02 (n = 12), and there were no further changes up to the last postnatal day studied, P29. In contrast to the myelinated CC, cortical gray matter remained isotropic up to P29, with a tortuosity of 1.54 ± 0.02 (n = 12). The results suggest that diffusion anisotropy in the rat CC is related to myelination; it reaches a maximum at P17, when myelination is well advanced. In myelinated pathways, preferential diffusion of ions and transmitters occurs along the axons. These results are relevant to volume transmission and the interpretation of diffusion-weighted magnetic resonance imaging.

INTRODUCTION

Extrasynaptic transmission plays an important role in short- and long-distance communication between neurons, axons, and glia. It is mediated by the diffusion of neuroactive substances, including ions and transmitters, through the extracellular space (ECS). In this way, transmitters can reach high-affinity receptors located outside synapses and often coupled to G proteins (Gilman 1987), as well as on glial cells (for review see Berger et al. 1995; Blankenfeld et al. 1995). This type of transmission is also called volume transmission, because the neuroactive substances and ions move through the volume of the ECS (Fuxe and Agati 1991). ECS is a communication channel whose size, structure, and composition determine the migration of molecules in the brain, i.e., the movement of substances by extracellular diffusion (Syková 1997). In principle, the structure of cellular aggregates and/or extracellular matrix can channel the migration of molecules in the ECS, so that diffusion in certain regions is facilitated in one direction rather than another. This could be a mechanism to allow a certain degree of specificity in volume transmission.

The real-time iontophoretic method using tetramethylammonium (TMA^+)-selective microelectrodes (Nicholson and Phillips 1981) can be used to determine the volume of the ECS, the so-called ECS volume fraction α (α = ECS volume/total tissue volume), and the tortuosity factor λ, which describes how the migration of molecules is slowed down by pore size, shape, and connectivity. Tortuosity describes the geometry of the ECS and is calculated from the measured TMA^+ diffusion coefficients as $\lambda = (D/\mathrm{ADC})^{0.5}$, where D is the free diffusion coefficient and ADC is the apparent diffusion coefficient of TMA^+ in brain tissue.

It has been shown that the diffusion properties of the ECS in brain (Lehmenkühler et al. 1993; McBain et al. 1990; Rice et al. 1993; Syková et al. 1996b) and spinal cord (Šimonová et al. 1996; Syková et al. 1994) are heterogeneous, i.e., they vary with anatomic structure and CNS region. Moreover, diffusion may be anisotropic, which means that the movement of substances even in homogeneous tissue, e.g., in white matter, is different in different directions.

With the use of the TMA^+ method, anisotropic diffusion has so far been demonstrated only in the molecular layer of the isolated turtle cerebellum (Rice at al. 1993). This in vitro study on a nonmammalian preparation examined a gray matter region with isotropic and anisotropic subregions. Anisotropic diffusion of water was described with the use of diffusion-weighted magnetic resonance imaging (MRI). It was shown that water diffusion is anisotropic in regions of white matter (Douek et al. 1991; Hajnal et al. 1991; Le Bihan et al. 1993; Moseley et al. 1990; Pierpaoli et al. 1996; Sakuma et al. 1991). However, it is not clear whether this anisotropy is due to anisotropic water diffusion in the ECS, because cell membranes are readily permeable to water and these measurements cannot distinguish between the intra- and extracellular compartments. The mechanisms responsible for the diffusion anisotropy in white matter are therefore far from clear.

To study diffusion anisotropy in the ECS in vivo, we measured TMA^+ diffusion in the rat cortex and corpus callosum (CC) during postnatal development. In contrast to water, cellular membranes are relatively inpermeable to TMA^+. Diffusion occurs in all directions and, with the use of the

TMA^+ method, we could measure it independently in three orthogonal axes (X, Y, and Z). The X-axis lies along the axons; the Y-axis and Z-axis lie across the fibers in CC. We addressed the question of whether anisotropic diffusion of substances in the ECS is related to gliogenesis and, particularly, myelination. Diffusion anisotropy in white matter ECS has not been studied previously, yet it is critical for MRI interpretation.

METHODS

Animal preparation

Experiments were performed on rat pups (Wistar strain) from postnatal day (P)4 to P29 (date of birth taken as P0) anesthetized with urethan (1.6–2.5 g/kg ip) and placed in a rat headholder. The body temperature was maintained at 36–37°C by supporting the rat on a heated, curved platform that enclosed the lower part of the body. The animals spontaneously breathed air. A hole, 2.0 mm diam, was made ~1.5 mm (P14–29) or 1 mm (P4–13) caudal from the bregma and ~2 mm lateral to the sutura medialis, and the dura was carefully removed. The exposed brain tissue was bathed in warmed (37°C) artificial cerebrospinal fluid (Lehmenkühler et al. 1993). Microelectrodes were introduced to the levels of cortical layer V and CC with the use of a remote control micromanipulator (Nanostepper, SPI, Oppenheim, Germany) and stereotaxic coordinates as described in our previous study (Lehmenkühler et al. 1993).

Ion-selective microelectrodes

Ion-selective microelectrodes (ISMs) were used to measure TMA^+ diffusion parameters in ECS. TMA^+-selective microelectrodes were prepared as described for K^+-selective electrodes (Kříž et al. 1974); the ion exchanger was Corning 477317, but the ion-sensing barrel was backfilled with 100 mM TMA chloride instead of 150 mM KCl. Electrodes were calibrated with the use of the fixed-interference method before and after each experiment in a sequence of solutions of 150 mM NaCl plus 3 mM KCl with the addition of the following concentrations of TMA chloride: 0.0003, 0.001, 0.003, 0.01, 0.03, 0.1, 0.3, 1.0, 3.0, and 10.0 mM.

For diffusion measurements, iontophoresis pipettes were prepared from theta glass (Clark Electrochemical Instruments, Pangbourne, UK). The shank was bent before backfilling with 0.5 M TMA chloride so that it could be aligned parallel to the ISM. Electrode arrays were made by gluing together an ISM and two iontophoresis pipettes, each with a tip separation of 110–180 μm from the tip of the ISM (Fig. 1). The tips of the three pipettes formed a 90° angle in a horizontal plane for measurements along the X- and Y-axes; for measurements along the Z-axis, one iontophoresis pipette tip was lowered 110–180 μm below the tip of the ISM. Typical iontophoresis parameters were +20-nA bias current (continuously applied to maintain a constant transport number), with a +200-nA current step 60 s in duration to generate the diffusion curve. The indifferent electode (Ag/AgCl wire) was placed in the muscle. Potentials recorded on the reference barrel of the ISM were subtracted from the ion-selective barrel voltage measurements by means of buffer and subtraction amplifiers.

Expression for anisotropic diffusion

The expected extracellular TMA^+ concentration, C, generated by iontophoresis in an anisotropic medium has been derived by Rice et al. (1993) as follows: when the iontophoresis pulse is applied for duration d, then $C = G(t)$ for the rising phase of the curve ($t < d$), and $C = G(t) - G(t - d)$ for the falling phase of the curve ($t \geq d$). The general expression for this function, $G(u)$, can be given as

$$G(u) = \frac{Q\lambda_x\lambda_y\lambda_z}{8\pi D\alpha r}\left[\exp\left(r\sqrt{\frac{k'}{D}}\right)\operatorname{erfc}\left(\frac{r}{2\sqrt{Du}} + \sqrt{k'u}\right) + \exp\left(-r\sqrt{\frac{k'}{D}}\right)\operatorname{erfc}\left(\frac{r}{2\sqrt{Du}} - \sqrt{k'u}\right)\right] \quad (1)$$

The parameter $r = (x^2\lambda_x^2 + y^2\lambda_y^2 + z^2\lambda_z^2)^{1/2}$, where x, y, and z are the distances in the rectangular Cartesian coordinates defined in Fig. 1. The source is defined by $Q = In/zF$, where I is the current applied to the iontophoresis electrode, n is the transport number of this electrode, z is the number of ionic charges on the ion, and F is Faraday's electrochemical equivalent. Nonspecific concentratration-dependent uptake is k' (Nicholson 1992; Nicholson and Philips 1981; Rice and Nicholson 1991). The function erfc is the complementary error function

$$\operatorname{erfc}(x) = \left(\frac{2}{\sqrt{\pi}}\right)\int_x^\infty \exp(-t^2)\,dt$$

To determine the five parameters λ_x, λ_y, λ_z, α, and k', measurements were made at the coordinates (x, 0, 0), (0, y, 0) and (0, 0, z) relative to the iontophoresis electrode at the origin (0, 0, 0). Then for (x, 0, 0)

$$G_x(u) = \frac{QA_x}{8\pi Dx}\left[\exp\left(x\lambda_x\sqrt{\frac{k'}{D}}\right)\operatorname{erfc}\left(\frac{x\lambda_x}{2\sqrt{Du}} + \sqrt{k'u}\right) + \exp\left(-x\lambda_x\sqrt{\frac{k'}{D}}\right)\operatorname{erfc}\left(\frac{x\lambda_x}{2\sqrt{Du}} - \sqrt{k'u}\right)\right] \quad (2A)$$

$$A_x = (\lambda_z\lambda_y/\alpha) \quad (2B)$$

similar expressions can be written down for $G_y(u)$, A_y and $G_z(u)$, A_z.

The parameters α_x, λ_x, and k' were determined from *Eq. 2A* with the use of a nonlinear curve fitting procedure (see next section); α_y, λ_y, k' and α_z, λ_z, k' were obtained similarly. The value of α could then be calculated with the use of *Eq. 2B* with averaged experimental data from each axis, and similar expressions for the other components. The three estimates of α and k' obtained with this method were not statistically significantly different and were therefore averaged to yield α and k' for layer V and CC. The anisotropy can be characterized by the three components of λ, here designated as λ_x, λ_y, and λ_z.

Measurements of ECS diffusion parameters

Concentration-versus-time curves for TMA^+ diffusion were first recorded in 0.3% agar gel (Difco, Special Noble Agar) made up in a solution composed of (in mM) 150 NaCl, 3 KCl, and 1 TMA^+ in a Lucite cup placed just above the brain. The array of electrodes was then lowered into the cortex to appropriate depths to coincide with the known distribution of gray mater–layer V and CC at various ages (Lehmenkühler et al. 1993).

A nonlinear curve-fitting simplex algorithm, implemented in the program VOLTORO (C. Nicholson, unpublished data) was used to fit *Eq. 1*, with $\alpha = 1$, $\lambda = 1$, and $k' = 0$, to determine the transport number (n) of the iontophoresis micropipette and the free diffusion coefficient, D, for TMA^+. After n was determined in agar gel, measurements were made in the brain to obtain α, λ_x, λ_y, λ_z, and k'. These parameters were extracted from the concentration-versus-time profiles by fitting *Eq. 2A* and *2B* and similar equations for the other axes with VOLTORO.

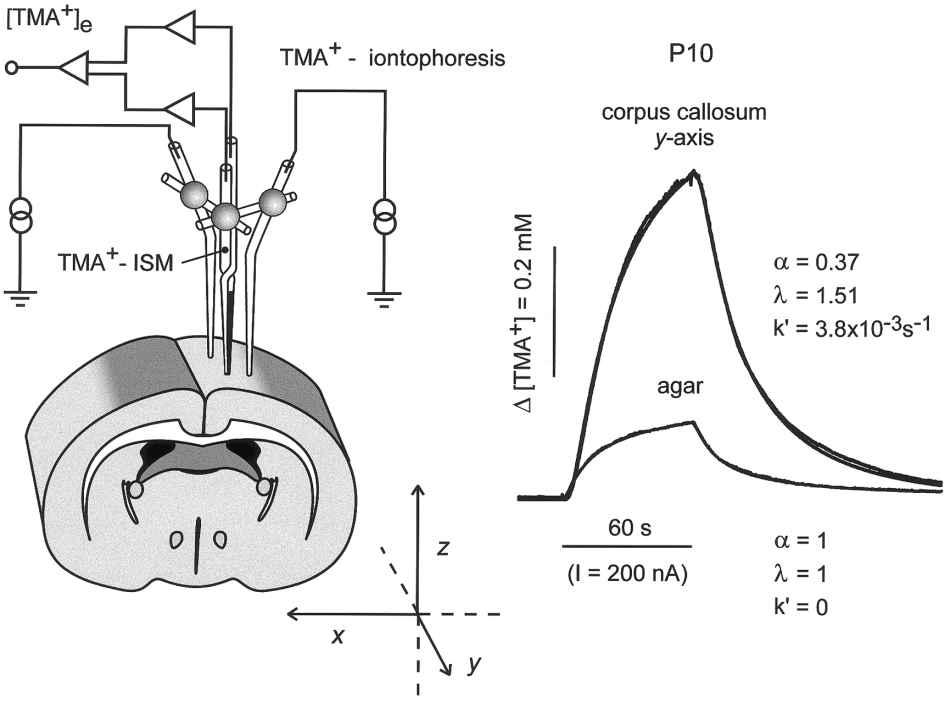

FIG. 1. Experimental setup and tetramethylammonium (TMA^+) diffusion curves. *Left*: schema of experimental arrangement. TMA^+-selective double-barreled ion-selective microelectrode (ISM) was glued to two bent iontophoresis microelectrodes. Separation between electrode tips was 110–180 μm. Tips of the 3 pipettes formed 90° horizontal angle for simultaneous measurements along *X*- and *Y*-axes. Similarly, for measurements along *Z*-axis, 1 iontophoresis pipette tip was lowered 110–180 μm below tip of ISM. When electrode array was inserted into corpus callosum and iontophoretic current was applied, diffusion curve resulting from increase in TMA^+ concentration was registered in *X*-, *Y*-, or *Z*-axis. *Right*: typical records obtained with this setup in agar gel and corpus callosum of animal at postnatal day (P)10. In this figure, as well as in Fig. 2, concentration scale is linear and theoretical diffusion curve (*Eq. 1*) is superimposed on each data curve. Values of volume fraction (α), tortuosity (λ), and nonspecific uptake (k') are shown with each record. Separation between ISM and iontophoresis electrode tip was 159 μm. Electrode transport number $n = 0.203$.

Statistical analysis and data processing

All data are presented as means ± SE. Statistical analysis of the differences between groups was evaluated by the Mann-Whitney test. Values of $P < 0.05$ were considered significant. Three-dimensional plots were made with the MATLAB version 4.2 program (MathWorks).

RESULTS

Diffusion parameters of the cortex and CC

Diffusion in nervous tissue is affected by α and λ, as is readily apparent from an inspection of the time course and amplitude of the TMA^+ diffusion curves in agar gel and brain (Fig. 1). The diffusion curves obtained in the cortex or CC have a greater amplitude than those in agar because the same amount of TMA^+ released from the iontophoretic electrode results in a greater increase in TMA^+ concentration in brain than in free medium because of the restricted ECS available for diffusion. TMA^+ diffusion curves in brain also rose more slowly than those in agar gel (Fig. 1), reflecting the reduction of the TMA^+ ADC in brain tissue and therefore an increase in λ (Nicholson 1992; Nicholson and Philips 1981).

TMA^+ diffusion curves recorded from the cortical gray matter and CC revealed distinct diffusion properties of these structures at the third postnatal week and later. Although the same diffusion curves were recorded from the *X*-, *Y*-, and *Z*-axes within the cortical layer V, different diffusion curves were recorded along each of the axes in CC (Fig. 2). As can be seen, preferential diffusion in white matter occurred along the myelinated axons.

Diffusion parameters during development

In previous papers, we showed that ECS volume decreases in gray matter in the first two, and in white matter in the first three, postnatal weeks to about one-half of its size at P2–3 while the tortuosity is essentially unchanged (Lehmenkühler et al. 1993; Syková et al. 1996b). Our measuments, however, were performed only along the *X*-axis and were correct only if one assumes that the diffusion in this developmental period is isotropic. Although this is the case in cortical gray matter, the present experiments revealed substantial anisotropy in white matter from about P13 and later. Two distinct age groups, P9–11 ($n = 6$) and P21–23 ($n = 6$), were selected for comparision and results are presented in Table 1. Table 1 shows that the diffusion in the cortex is isotropic in both age groups, whereas in CC, diffusion is isotropic in animals at P9–11 and anisotropic at P21–23. At P21–23, a significant difference ($P < 0.001$) was found between λ_x and λ_y values and between λ_x and λ_z values. Although the tortuosity along the *X*-axis (i.e., parallel to the axons) remains the same from P4 to P29, the λ values in both *Y* and *Z* axes (i.e., across the axons) gradually increase from P13 to reach their maximal values at P17 (Fig. 3). This time course of tortuosity increase across the axon fibers correlates with CC myelination (Bjartmar 1996; Hamano et al. 1996).

We previously reported that the decrease in α during postnatal development is faster in gray than in white matter. In the present study, more detailed measurements confirm this finding, but show that the decrease in white matter is faster than we could predict from measurements along the *X*-axis only (Lehmenkühler et al. 1993). Importantly, the decrease in α was already observed at P5 and therefore preceeds the increase in λ_y and λ_z by ≥7 days (Fig. 3). The values of α at P21–120 (0.19–0.20) described in myelinated CC by Lehmenkühler et al. (1993) are lower than the true values of α found in this study (0.26), now obviously calculated from three measured λ values (*x*, *y*, and *z*, Table 1).

The values of α in the gray matter and CC at P9–11 are

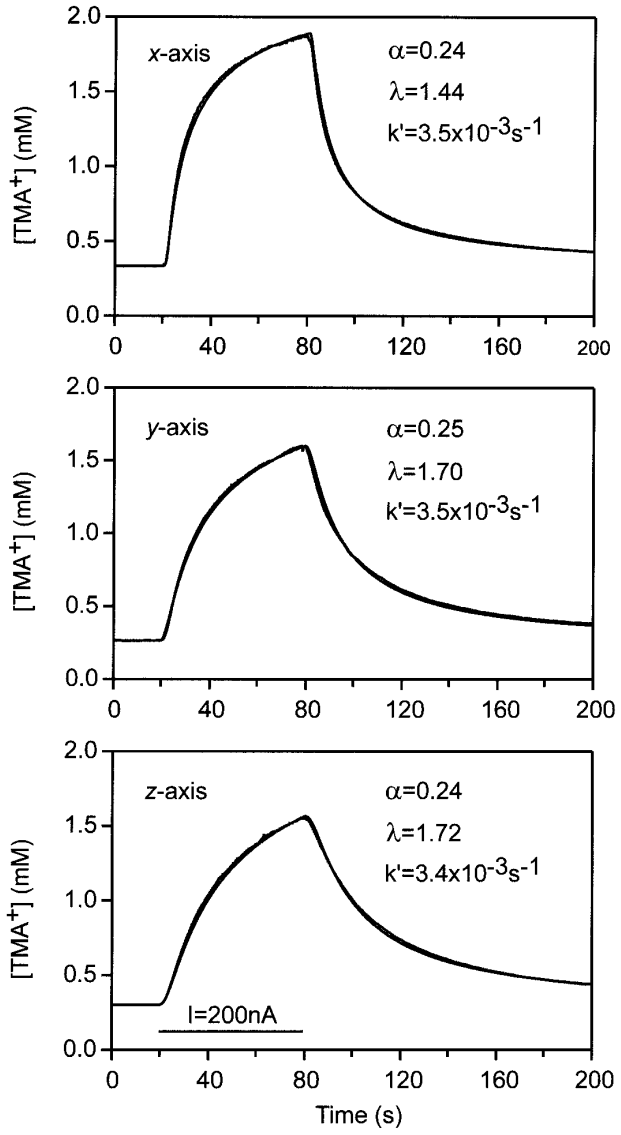

FIG. 2. Representative records obtained in corpus callosum in *X*-axis (along axons) and in *Y*- and *Z*-axes (across axons). All recordings are from same animal at P21 and were recorded with 2 microelectrode arrays. Values of α, λ, and k' are shown with each curve. Recordings were first made with microelectrode array in *X*- and *Y*-axes (array spacing in *X*-axis was 132 μm and $n = 0.352$; in *Y*-axis, 140 μm and $n = 0.339$). Second microelectrode track was made with array fixed in *Y*- and *Z*-axes. Values obtained in *Y*-axis were same as those obtained with first array (not shown). In *Z*-axis, microelectrode spacing was 137 μm and $n = 0.335$. Shape and amplitude of diffusion curves reflect different diffusion coefficients along each of the selected axes.

different, which is an indication of diffusion heterogeneity during development (Table 1). The mean value of α calculated with the use of the appropriate form of *Eq. 2* was 0.27 in gray matter, whereas in CC it was 0.36, significantly different from that of gray matter ($P < 0.01$). At P21–23, the mean value of α was 0.23 in gray matter and 0.26 in CC, i.e., the significant difference in α value between gray and white matter persisted ($P < 0.05$).

The nonspecific linear uptake, k', is, like α, a scalar quantity, and therefore has a single value in all three axes. The uptake significantly increased as the animals aged (Fig. 3).

Isoconcentration ellipsoids

The three-dimensional pattern of diffusion away from a point source can be illustrated by constructing iso-concentration spheres (isotropic diffusion) and ellipsoids (anisotropic diffusion) for extracellular TMA^+ concentration (Fig. 4). The surfaces in Fig. 4 represent the locations where TMA^+ concentration first reached 1 mM, 10 s after the initiation of a 200-nA iontophoresis current. The value of r for which $G(t)$ was equal to 1 mM was found graphically by solving *Eq. 1* and *2*. We used the mean values for λ_x, λ_y, and λ_z given in Table 1 together with the following parameters: $D = 1.311 \times 10^{-5}$ cm^2/s at 37°C, $n = 0.300$, and $k' = 4.0 \times 10^{-3}$ s^{-1}. The three-dimensional plots were then generated from the expression $Z = (r^2 - x^2\lambda_x^2 - y^2\lambda_y^2)^{1/2}/\lambda_z$ derived from the definition of r (Rice et al. 1993). The single values for r, which describe the equivalent spheres determined by this procedure, were 36 μm for the agar gel, 102 and 117 μm for gray matter at P6 and P21, respectively, and 92 μm for CC at P6. The tiny sphere representing diffusion in agar gel (Fig. 4) shows the dramatic difference between a free medium and constrained diffusion in the brain. Figure 4 also shows that the larger the ECS value, the smaller the sphere. The spherical surface in gray matter and CC at P6 reflects the ability of particles to diffuse equaly along the *X*-, *Y*-, and *Z*-axes of these structures. In CC at P21, the r_x and $r_{y,z}$ describing the equivalent ellipsoids were 130 and 107, respectively. The ellipsoidal surface in Fig. 4 reflects the different abilities of substances to diffuse along the *X*-, *Y*-, and *Z*-axes of the myelinated CC.

DISCUSSION

Structural anisotropy of the ECS

To characterize anisotropy of mammalian ECS, we studied extracellular diffusion in the rat CC and layer V of the somatosensory neocortex. These regions were selected because the axons in CC are myelinated and oriented in parallel, and therefore should constrain diffusion. On the other hand, layer V of the cortex is rich with cell bodies, dendrites, and axons that have no preferential orientation, and therefore the diffusion might be rather isotropic. To find out whether axon fiber orientation and/or myelination plays a crucial role in white matter anisotropy, we investigated rats at different ages. At P4–6 the axons in rat CC are largely unmyelinated (Hamano et al. 1996) although already oriented in parallel; at P12 about two-thirds of the axonal length is still unsheathed, whereas at P17 only ~20% is unsheathed (Bjartmar 1996; Hildebrand et al. 1993). Hamano et al. (1996) found that the intensity of myelination in rat CC quickly increases between P14 and P21 but does not significantly increase after about P21. Indeed, this corresponds well with our findings that below P13 there is no anisotropic TMA^+ diffusion in CC and above P17 there in no further significant increase in anisotropy (see Fig. 3). Our data therefore show that diffusion in the ECS of unmyelinated axon bundles is isotropic. Because TMA^+ diffuses almost solely through the ECS (see also very low uptake in unmyelinated as well as in myelinated CC), the myelin sheaths apparently slow down the diffusion around the axons but have no effect on diffusion in the ECS along the axons.

TABLE 1. *Comparison of λ, α, and k′ in the corpus callosum and cortical gray matter (layer V)*

	P9–11		P21–23	
	Corpus callosum	Gray matter	Corpus callosum	Gray matter
λ_x	1.49 ± 0.03	1.56 ± 0.01	1.46 ± 0.03	1.54 ± 0.02
λ_y	1.53 ± 0.2	1.55 ± 0.02	1.70 ± 0.01	1.54 ± 0.02
λ_z	1.54 ± 0.02	1.56 ± 0.02	1.72 ± 0.02	1.55 ± 0.01
α	0.36 ± 0.01	0.27 ± 0.01	0.26 ± 0.01	0.23 ± 0.02
k' ($\times 10^3$ s^{-1})	3.6 ± 0.2	3.4 ± 0.4	5.0 ± 0.4	4.8 ± 0.5

Shown are 2 distinct age groups, postnatal day (P)9–11 and P21–23. Values for tortuosity (λ_x, λ_y, λ_z), volume fraction (α) and nonspecific uptake (k') are means ± SE (n = 12 measurements, 6 animals for each). Individual records were analyzed using *Eq. 1* and *2*.

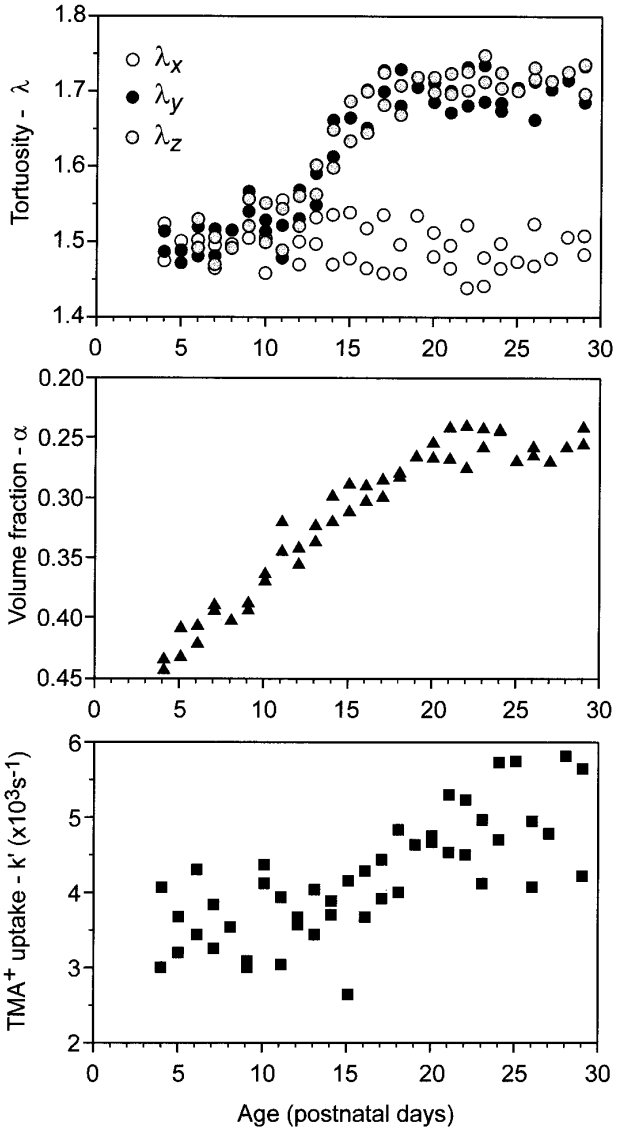

FIG. 3. Diffusion anisotropy during development. Rat pups from P4 to P29 were used, 2 animals at every given age except P19, P25, P27, and P28, where only 1 animal was used. Values of α in corpus callosum decreased before or at P4 and reached stable values at about P20. λ Stayed constant in *X*-axis. λ Values in *Y*- and *Z*-axes up to P12 were same as in *X*- axis, but λ_y and λ_z started to increase at about P13. After P13, λ_y and λ_z gradually increased and reached maximum values at P17, then remained constant.

Our finding that ECS volume clearly decreases before myelination suggests that the anisotropy is not the result of a more compacted ECS in myelinated CC. Moreover, the smaller ECS volume in cortex (0.23) as compared with CC (0.26) is not accompanied by an increase in the λ values. We therefore conclude that as glia mature in the first postnatal week, these developing cellular elements cause a decrease in α, without altering λ. The lack of anisotropy at this stage can be explained by the absence of directionality in the developing glial cells. In contrast, the beginning of myelination results in the maturation of a structural component that does have directionality, and thus the tissue becomes increasingly anisotropic. In this case, λ increases in directions perpendicular to the myelinated fibers, because diffusing molecules have to go around those fibers in the *Y* and *Z* directions, whereas in the *X* direction, the molecules simply go along the fibers so that the tortuosity is comparatively lower (Fig. 5). Our model in Fig. 5, which is based on present TMA^+ diffusion data and immunohistochemical studies (Bjartmar 1996; Hamano et al. 1996) furthermore suggests that not only the number of myelin sheaths but also the length of myelin sheaths versus unmyelinated axon parts might be important for the extracellular tortuosity increase and CC anisotropy observed with the TMA^+ method.

Structural anisotropy in some regions of the brain has also been inferred from impedance measurements and MRI. Neither impedance (Garden-Medwin 1980) nor MRI (Moseley et al. 1990) can, however, distinguish between the intra- and extracellular compartments, and therefore these studies could not confirm the extent of anisotropy in the ECS. Many recent MRI studies of water diffusion reveal anisotropy in ADC_W in the white matter of mammals and humans (Chenevert et al. 1990; Doran et al. 1990; Douek et al. 1991; Hajnal et al. 1991; Moseley et al. 1990; Pierpaoli and Basser 1996). The diffusion of water in myelinated white matter was shown to be 3 times (Le Bihan et al. 1995) or even 10 times (Pierpaoli and Basser 1996) faster along the myelin fiber direction than perpendicular to the fibers. When these water diffusion studies are compared with our TMA^+ diffusion measurements describing purely extracellular diffusion parameters, there are some important differences. Some of the MRI studies demonstrated that the diffusion anisotropy is more distinct after brain maturation and myelination (Chenevert et al. 1990) and that the diffusion anisotropy was closely related to the development of white matter (Sakuma et al. 1991). In several studies, however, a decrease in ADC_W across the fibers was reportedly found in unmyelin-

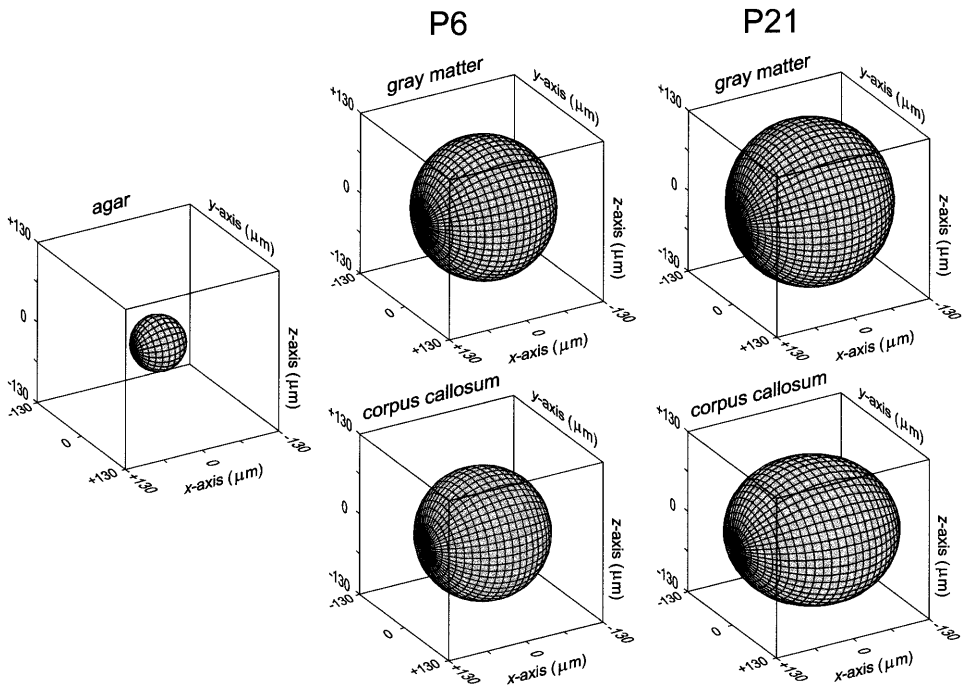

FIG. 4. Diffusion spheres in agar, cortical layer V (gray matter), and corpus callosum in animals at P6 and P21. Isoconcentration surfaces for 1 mM TMA^+ concentration contour 10 s after onset of 200-nA iontophoretic pulse reveal spherical diffusion in agar gel and isotropic diffusion in cortical gray matter and corpus callosum at P6. Anisotropic diffusion was found in corpus callosum at P21 (ellipsoidal surface). Surfaces were generated as described in text with the use of measured values for λ_x, λ_y, λ_z, and α in given experiment. n, α, $\lambda_{x,y,z}$, and k' ($\times 10^{-3}$ s^{-1}) in diffusion measurments in brain were as follows: P6, gray matter—0.367, 0.35, 1.55, 3.3; P6, corpus callosum—0.367, 0.44, 1.51, 3.8; P21, gray matter—0.342, 0.23, 1.56, 4.8 and P21, corpus callosum—values as in Fig. 2. For all measurements, $D = 1.311 \times 10^{-5}$ cm^2/s; n in agar = 0.352.

ated tissue (Ono et al. 1995) or preceeding myelination (Wimberger et al. 1995). This has been explained by anisotropic water diffusion in anisotropic tissue (including unmyelinated tissue) because the extracellular diffusion of water is retarded by cell membranes (Basser et al. 1994), or the anisotropy can be due to different intrinsic properties of axoplasm so that intracellular water diffusion can be hindered by microtubules or neurofilaments, or the water diffusion can be actively facilitated by axoplasmatic transport or bulk flow in ECS (Le Bihan et al. 1993). If it is true that water diffusion is anisotropic even in unmyelinated tissue, anisotropic diffusion could be used to determine nerve fiber tract orientation noninvasively in vivo, with the use of diffusion-weighted MRI (Basser et al. 1994). However, some of the MRI studies (Wimberger et al. 1995) that report anisotropy in white matter before the onset of myelination did not employ sensitive immunohistochemical methods. Wimberger et al. (1995) report that the onset of anisotropic magnetic resonance signal occurs at P18–20, but they report that CC myelination was first visible in rats at P26–28 with the use of staining with Luxol fast blue and Holmes silver nitrate. This is apparently an underestimation; to show the beginning and extent of myelination one should probably use antibodies directed against myelin proteins, i.e., myelin

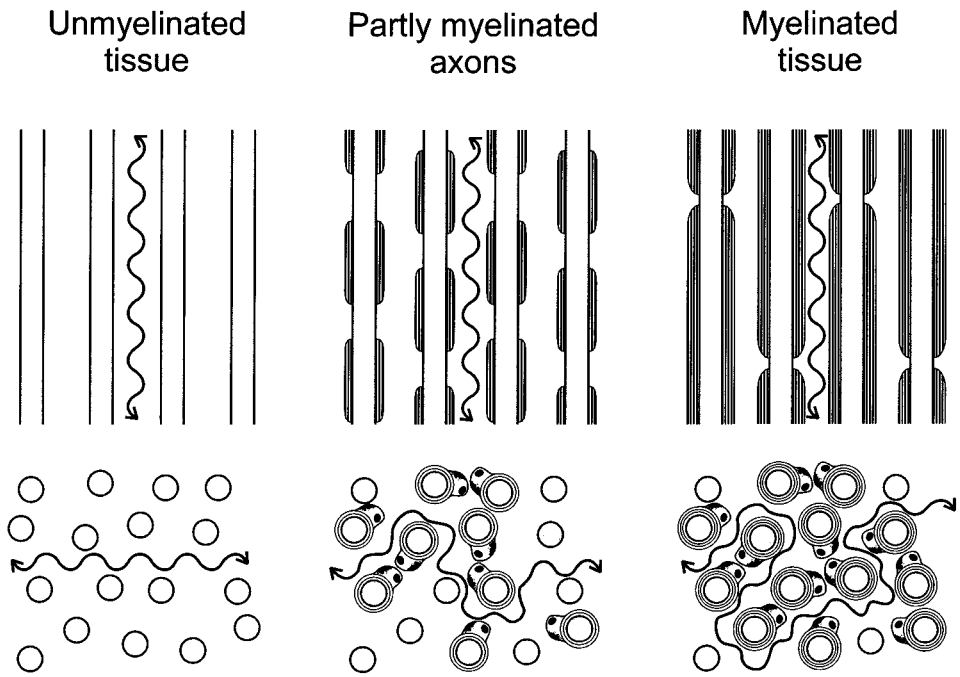

FIG. 5. Diffusion in extracellular space of unmyelinated, partly myelinated, and myelinated corpus callosum. *Top*: diffusion along increasingly myelinated axons is not affected by decrease in extracellular space α up to ~50%. *Bottom*: extracellular diffusion in direction perpendicular to orientation of axons, i.e., around axons, is compromised by number of myelin sheaths, number of myelinated axons, and length of myelin sheaths along axons. Scheme demonstrates increased anisotropy as myelination progresses.

basic protein (MBP) or proteolipid protein, which reveal that myelination starts much earlier, before P14, and that at P21 CC is extensively myelinated (Hamano et al. 1996; Yamada et al. 1996).

One might speculate that the packing density of fibers would contribute to the measured TMA^+ and/or water diffusion anisotropy. Hajnal et al. (1991) reported that the packing density of fibers in white matter tracts varies tenfold and suggested that tracts with lower packing density also have a lower anisotropy. However, this has not been proven to be the case in human brain, taking into account the packing density of fibers as well as the packing density of glial cells (Pierpaoli and Basser 1996; Pierpaoli et al. 1996). In the present study we show that a significant decrease in the ECS volume fraction occurs before myelination from P4 to P12, yet the ADC_{TMA} and tortuosity are not changing and diffusion is isotropic.

In light of our study, it is hard to believe that myelination would not substantially slow down the diffusion of water in the direction perpendicular to the orientation of myelinated axons, because myelin is 10–50 times less permeable to water than unmyelinated membranes (Finkelstein 1987). It is, however, a question whether the anisotropy in water diffusion is linearly proportional to the number of myelin sheaths. This might be true for water but not for other molecules diffusing in the ECS, including TMA^+. It is also possible that it is not the number of myelinated axons and/or the number of myelin sheaths, but rather the length of myelin sheaths along the myelinated axon versus the length of unmyelinated axon, that is of particular importance for the anisotropy of water diffusion.

Nature of tortuosity increase in white matter

Tortuosity is a geometric parameter that incorporates many factors we presently cannot determine as separate entities. These might be: membrane barriers including neuronal and glial processes, myelin sheaths, macromolecules including the molecules of the extracellular matrix, molecules with fixed negative surface charges, ECS size, and pore geometry. Our recent studies support the role of geometric constraints, because the increase in tortuosity accompanies astrogliosis (Roitbak et al. 1996; Syková et al. 1996a,b), myelination in grafted tissue (Roitbak et al. 1996), and a rise in the macromolecular content of the extracellular fluid (Tao and Nicholson 1996). On the other hand, changes in ECS size during development are not accompanied by an increase in tortuosity (Lehmenkühler et al. 1993). The importance of the tortuosity increase due to myelination and not fiber packing is also supported by the fact that the developmental decrease in ECS volume in CC (Fig. 3) has a different time course than myelination and the occurrence of anisotropic diffusion of TMA^+. Our model in Fig. 5 also shows that diffusion along the axons might not be more hindered, because the size of the space between axons is still large enough not to affect TMA^+ diffusion along the axons. Our data show that the three distinct values of λ in anisotropic tissue result from geometric diversity rather than from changes in the size of the ECS.

Functional significance of anisotropic diffusion

The functional relevance of anisotropic diffusion in the cerebellar molecular layer was demonstrated by the effect of the putative parallel fiber transmitter glutamate on ion shifts (K^+ and Ca^{2+}) along the *X*- and *Y*-axes; about a twofold greater increase in extracellular K^+ and decrease in extracellular Ca^{2+} was found in the *X*-axis along the parallel fibers after iontophoretic application of glutamate (Rice et al. 1993). Although these results are preliminary, this suggests that anisotropic diffusion may play an important role in the action of extrasynaptic glutamatergic transmission. Our recent data also show that cellular swelling induced by an application of hypotonic solutions or 50 mM K^+ results in different geometric changes, even when ECS volume decreased to the same level (the 3 tortuosity values were not affected by the same magnitude) (Prokopová and Syková 1997).

ECS represents the pathway for volume transmission and for intercellular, particularly neuron-glia, communication. ECS diffusion parameters, including anisotropy, may help to limit the diffusion of transmitters to regions occupied by their high-affinity receptors, located extrasynaptically and often coupled to G proteins (Gilman 1987). In addition, ECS diffusion parameters affect the diffusion of other neuroactive substances and ions during physiological and pathological states. The anisoptropy of the ECS in CC and in some other brain areas including cerebellum (Rice et al. 1993), hippocampus (E. Syková and T. Mazel, unpublished data) and neostriatum (Bjelke et al. 1995) may allow for some specificity as well as for new modes of extrasynaptic transmission by diffusion.

This work was supported by Grant Agency of the Czech Republic Grants 309/96/0884, 307/96/K226, and 309/97/K048 and Internal Grant Agency of the Ministry of Health, Czech Republic, Grants 3423-3 and 9517.

Address for reprint requests: E. Syková, Institute of Experimental Medicine, Academy of Science of the Czech Republic, Vídeňká 1083, Prague 142 20, Czech Republic.

Received 11 February 1997; accepted in final form 21 April 1997.

REFERENCES

BASSER, P. J., MATTIELLO, J., AND LE BIHAN, D. MR diffusion tensor spectroscopy and imaging. *Biophys. J.* 66: 259–267, 1994.

BERGER, T., MULLER, T., AND KETTENMANN, H. Developmental regulation of ion channels and receptors on glial cells. *Perspect. Dev. Neurobiol.* 2: 347–356, 1995.

BJARTMAR, C. Oligodendroglial sheath lengths in developing rat ventral funiculus and corpus callosum. *Neurosci. Lett.* 216: 85–88, 1996.

BJELKE, B., ENGLAND, R., NICHOLSON, C., RICE, M. E., LINDBERG, J., ZOLI, M., AGNATI, L. F., AND FUXE, K. Long distance pathways of diffusion for dextran along fibre bundles in brain. Relevance for volume transmission. *Neuroreport* 6: 1005–1009, 1995.

BLANKENFELD, G., ENKVIST, K., AND KETTENMANN, H. Gamma-aminobutyric acid and glutamate receptors. In: *Neuroglia*, edited by H. Kettenmann and B. R. Ransom. New York: Oxford Univ. Press, 1995, p. 335–345.

CHENEVERT, T. L., BRUNBERG, J. A., AND PIPE, J. G. Anisotropic diffusion in human white matter: demonstration with MR techniques in vivo. *Radiology* 177: 401–405, 1990.

DORAN, M., HAJNAL, J. V., VAN BRUGGEN, N., KING, M. D., YOUNG, I. R., AND BYDDER, G. M. Normal and abnormal white matter tracts shown by MR imaging using directional diffusion weighted sequences. *J. Comput. Assist. Tomogr.* 14: 865–873, 1990.

DOUEK, P., TURNER, R., PEKAR, J., PATRONAS, N., AND LE BIHAN, D. MR

color mapping of myelin fiber orientation. *J. Comput. Assist. Tomogr.* 15: 923–929, 1991.

FINKELSTEIN, A. *Water Movement Through Lipid Bilayers, Pores and Plasma Membranes: Theory and Reality.* New York: Wiley, 1987.

FUXE, K. AND AGNATI, L. F. *Volume Transmission in the Brain.* New York: Raven, 1991.

GARDEN-MEDWIN, A. R. Membrane transport and solute affecting the brain cell microenviroment. *Neurosci. Res. Prog. Bull.* 18: 208–226, 1980.

GILMAN, A. G. G proteins: transducers of receptor-generated signals. *Annu. Rev. Biochem.* 56: 615–649, 1987.

HAJNAL, J. V., DORAN, M., HALL, A. S., COLLINS, A. G., OATRIDGE, A., PENNOCK, J. M., YOUNG, I. R., AND BYDDER, G. M. MR imaging of anisotropically restricted diffusion of water in the nervous system: technical, anatomic, and pathologic considerations. *J. Comput. Assist. Tomogr.* 15: 1–18, 1991.

HAMANO, K., IWASAKI, N., TAKEYA, T., AND TAKITA, H. A quantitative analysis of rat central nervous system myelination using the immunohistochemical method for MBP. *Dev. Brain Res.* 93: 18–22, 1996.

HILDEBRAND, C., REMAHL, S., PERSSON, H., AND BJARTMAR, C. Myelinated nerve fibers in the CNS. *Prog. Neurobiol.* 40: 319–384, 1993.

KŘÍŽ, N., SYKOVÁ, E., UJEC, E., AND VYKLICKÝ, L. Changes of extracellular potassium concentration induced by neuronal activity in the spinal cord of the cat. *J. Physiol. Lond.* 238: 1–15, 1974.

LE BIHAN, D., TURNER, R., AND DOUEK, P. Is water diffusion restricted in human brain white matter? An echo-planar NMR imaging study. *Neuroreport* 4: 887–890, 1993.

LE BIHAN, D., TURNER, R., AND PATRONAS, N. Diffusion MR imaging in normal brain and in brain tumors. In: *Diffusion and Perfusion Magnetic Resonance Imaging*, edited by D. Le Bihan. New York: Raven, 1995, p. 134–140.

LEHMENKÜHLER, A., SYKOVÁ, E., SVOBODA, J., ZILLES, K., AND NICHOLSON, C. Extracellular space parameters in the rat neocortex and subcortical white matter during postnatal development determined by diffusion analysis. *Neuroscience* 55: 339–351, 1993.

MCBAIN, C. J., TRAYNELIS, S. F., AND DINGLEDINE, R. Regional variation of extracellular space in the hippocampus. *Science Wash. DC* 249: 674–677, 1990.

MOSELEY, M. E., COHEN, Y., KUCHARCZYK, J., MINTOROVITCH, J., ASAGARI, H. S., WENDLAND, M. F., TSURUDA, J., AND NORMAN, D. Diffusion-weighted MR imagining of anisotropic water diffusion in cat central nervous system. *Radiology* 176: 439–445, 1990.

NICHOLSON, C. Quantitative analysis of extracellular space using the method of TMA^+ iontophoresis and the issue of TMA^+ uptake. *Can. J. Physiol. Pharmacol.* 70, *Suppl.*: 314–322, 1992.

NICHOLSON, C. AND PHILIPS, J. M. Ion diffusion modified by volume fraction and tortuosity in the extracellular microenvironment of the rat cerebellum. *J. Physiol. Lond.* 321: 225–257, 1981.

ONO, J., HARADA, K., TAKAHASHI, M., MAEDA, M., IKENAKA, K., SAKURAI, K., SAKAI, N., KAGAWA, T., FRITZ-ZIEROTH, B., NAGAI, T., NIHEI, A., HASHIMOTO, S., AND OKADA, S. Differentiation between dysmyelination and demyelination using magnetic resonance diffusional anisotropy. *Brain Res.* 671: 141–148, 1995.

PIERPAOLI, C. AND BASSER, P. J. Toward a quantitative assessment of diffusion anisotropy. *Magn. Reson. Med.* 36: 893–906, 1996.

PIERPAOLI, C., JEZZARD, P., BASSER, P. J., BARNETT, A., AND DI CHIRO, G. Diffusion tensor MR imaging of the human brain. *Radiology* 201: 637–648, 1996.

PROKOPOVÁ, Š. AND SYKOVÁ, E. Diffusion anisotropy in white matter of the rat spinal cord: effects of potassium and hypotonic solutions (Abstract). *Physiol. Res.* In press.

RICE, M. E. AND NICHOLSON, C. Diffusion characteristics and extracellular volume fraction during normoxia and hypoxia in slices of rat neostriatum. *J. Neurophysiol.* 65: 264–272, 1991.

RICE, M. E., OKADA, Y. C., AND NICHOLSON, C. Anisotropic and heterogeneous diffusion in the turtle cerebellum: implications for volume transmission. *J. Neurophysiol.* 70: 2035–2044, 1993.

ROITBAK, T., MAZEL, T., ŠIMONOVÁ, Z., HARVEY, A., AND SYKOVÁ, E. Extracellular space volume and geometry in rat fetal brain grafts (Abstract). *Eur. J. Neurosci.* 9, Suppl.: 37, 1996.

SAKUMA, H., NOMURA, Y., TAKEDA, K., TAGAMI, T., NAKAGAWA, T., TAMAGAWA, Y., ISHII, Y., AND TSUKAMOTO, T. Adult and neonatal human brain: diffusional anisotropy and myelination with diffusion-weighted MR imaging. *Radiology* 180: 229–233, 1991.

ŠIMONOVÁ, Z., SVOBODA, J., ORKAND, P., BERNARD, C.C.A., LASSMANN, H., AND SYKOVÁ, E. Changes of extracellular space volume and tortuosity in the spinal cord of Lewis rats with experimental autoimmune encephalomyelitis. *Physiol. Res.* 45: 11–22, 1996.

SYKOVÁ, E. The extracellular space in the CNS: its regulation, volume and geometry in normal and pathological neuronal function. *Neuroscientist* 3: 334–347, 1997.

SYKOVÁ, E., MAZEL, T., AND ROITBAK, T. Extracellular space diffusion parameters in the rat brain during aging. *Soc. Neurosci. Abstr.* 22: 1495, 1996a.

SYKOAVÁ, E., SVOBODA, J., POLÁK, J., AND CHVÁTAL, A. Extracellular volume fraction and diffusion characteristics during progressive ischemia and terminal anoxia in the spinal cord of the rat. *J. Cereb. Blood Flow Metab.* 14: 301–311, 1994.

SYKOVÁ, E., SVOBODA, J., ŠIMONOVÁ, Z., LEHMENKÜHLER, A., AND LASSMANN, H. X-irradiation-induced changes in the diffusion parameters of the developing rat brain. *Neuroscience* 70: 597–612, 1996b.

TAO, L. AND NICHOLSON, C. Diffusion of albumins in rat cortical slices and relevance to volume transmission. *Neuroscience* 75: 839–847, 1996.

WIMBERGER, D. M., ROBERTS, T. P., BARKOVICH, A. J., PRAYER, L. M., MOSELEY, M. E., AND KUCHARCZYK, J. Identification of ''premyelination'' by diffusion-weighted MRI. *J. Comput. Assist. Tomogr.* 19: 28–33, 1995.

YAMADA, M., KAGAWA, T., AND IKENAKA, K. Development and differentiation of oligodendrocytes. *Jpn. J. Physiol.* 46: 105–110, 1996.